A Myosin I Is Involved in Membrane Recycling from Early Endosomes

Eva M. Neuhaus and Thierry Soldati

Department of Molecular Cell Research, Max-Planck-Institute for Medical Research, D-69120 Heidelberg, Germany

Abstract. Geometry-based mechanisms have been proposed to account for the sorting of membranes and fluid phase in the endocytic pathway, yet little is known about the involvement of the actin–myosin cytoskeleton. Here, we demonstrate that *Dictyostelium discoideum* myosin IB functions in the recycling of plasma membrane components from endosomes back to the cell surface. Cells lacking MyoB (*myoA*$^-$*/B*$^-$, and *myoB*$^-$ cells) and wild-type cells treated with the myosin inhibitor butanedione monoxime accumulated a plasma membrane marker and biotinylated surface proteins on intracellular endocytic vacuoles. An assay based on reversible biotinylation of plasma membrane proteins demonstrated that recycling of membrane components is severely impaired in *myoA/B* null cells. In addition, MyoB was specifically found on magnetically purified early pinosomes. Using a rapid-freezing cryoelectron microscopy method, we observed an increased number of small vesicles tethered to relatively early endocytic vacuoles in *myoA*$^-$*/B*$^-$ cells, but not to later endosomes and lysosomes. This accumulation of vesicles suggests that the defects in membrane recycling result from a disordered morphology of the sorting compartment.

Key words: *Dictyostelium* • endocytosis • membrane recycling • myosins • sorting

Introduction

A central problem encountered at each step of the trafficking between intracellular compartments is the effective sorting of membrane components from fluid phase, and of exported proteins from residents. Besides well-characterized signal-based mechanisms, models have been proposed in which the sorting of membrane from fluid phase is achieved on a geometric basis by modulating the surface to volume ratio of the sorting compartments (Linderman and Lauffenburger, 1988; Dunn et al., 1989). The role of the cytoskeleton in achieving, regulating, and maintaining the morphology of intracellular compartments, thereby forming the mechanical support for geometry-based sorting processes, has only recently been considered.

A central task of the endocytic pathway is the triage of ingested fluid from membrane-bound molecules (Gruenberg and Maxfield, 1995). Although the recycling of most membrane-bound molecules does not require any specific signal, this process is rendered very efficient through the use of small vesicles or tubules with high surface to volume ratio (Mayor et al., 1993; Verges et al., 1999). The kinetics of receptor recycling consists of distinct fast and slow components, indicating that recycling occurs from two different endosomal compartments (Sheff et al., 1999).

Address correspondence to Thierry Soldati, Department of Molecular Cell Research, Max-Planck-Institute for Medical Research, Jahnstrasse 29, D-69120 Heidelberg, Germany. Tel.: 49-6221-486407. Fax: 49-6221-486325. E-mail: soldati@mpimf-heidelberg.mpg.de

During their lifetime, vesicles mediating membrane traffic have to successively recruit the machineries necessary for their formation, their transport, and the selection, tethering, docking, and, finally, fusion with their target membrane. The membrane trafficking machinery has to be coordinated with the cytoskeleton to ensure both efficient and rapid formation of tubular/vesicular structures and the delivery to distant target compartments (Schroer, 2000). The role of microtubules and associated motor proteins, kinesin and dynein, has been extensively investigated in the last years (Hirokawa, 1998). More recently, the importance of the actin cytoskeleton in the proper working of many steps of the secretory and endocytic pathways is becoming apparent.

Filamentous actin is involved in the endocytosis of fluid phase markers from the apical (Gottlieb et al., 1993) and basolateral membrane of polarized cells (Shurety et al., 1998). An involvement of actin in receptor-mediated endocytic uptake processes was shown in yeast (Kubler and Riezman, 1993) and mammalian cells (Durrbach et al., 1996; Lamaze et al., 1997), though its role may be not obligatory in mammalian cells (Fujimoto et al., 2000). Actin was shown to localize also to sorting endosomes in fibroblasts (Nakagawa and Miyamoto, 1998). The ADP-ribosylation factor (ARF)-6 GTPase, which was shown to be important in modeling the plasma membrane and cortical actin cytoskeleton (Song et al., 1998), was recently implicated in the targeted delivery of recycling en-

dosomal vesicles to the plasma membrane (D'Souza-Schorey et al., 1998). Despite accumulating evidence for interactions between actin and coat proteins (Kohtz et al., 1990; Gaidarov et al., 1999), much less is known about the involvement of actin-dependent motor proteins. The discovery of a great diversity of myosins associated with many different organelles suggests that, in addition to bona fide transport, the actomyosin cytoskeleton may play a role in sorting processes and the modulation of membrane structures (Coluccio, 1997).

At least four classes of myosins, I, II, V, and VI, have been directly involved in membrane trafficking (for review see Mermall et al., 1998). Among these, the double-headed myosin V and myosin VI were shown to transport organelles and particles along actin filaments. Evidence also exists for involvement of myosins in budding of vesicles from intracellular compartments. Nonmuscle myosin II in mammalian cells is recruited to Golgi membranes with features of a coat protein during the budding of transport vesicles (Müsch et al., 1997; Stow et al., 1998). Class I myosins are involved in different aspects of endocytic processes (Tuxworth and Titus, 2000). It was proposed that they act at later stages of vesicle formation, like the fission of the endocytic vesicles from the plasma membrane or from internal vacuoles, or power the movement of newly formed vesicles through the cortical actin meshwork (Ostap and Pollard, 1996). Myo5 and Myo3, the yeast class I myosins, are required for receptor-mediated endocytosis, possibly for a budding event in the uptake process (Goodson and Spudich, 1995; Geli and Riezman, 1996). Homologues of these myosins are implicated in endocytosis in many other organisms and may execute a variety of similar tasks. Myosin IB from *Dictyostelium discoideum* (Jung and Hammer, 1990; Wessels et al., 1991), *Acanthamoeba castellanii* (Jung et al., 1989), and *Entamoeba histolytica* (Vargas et al., 1997) as well as myosin IA from *Aspergillus nidulans* (McGoldrick et al., 1995) show highest homology to both Myo5p and Myo3p and somehow participate in endocytic mechanisms. *D. discoideum* double deletion mutants (*myoA*$^-$/*myoB*$^-$ and *myoC*$^-$/*myoB*$^-$) show conditional defects in fluid phase pinocytosis (Novak et al., 1995; Jung et al., 1996). Other types of class I myosins also function in the endocytic pathway. For example, mammalian myosin Iα is associated with endosomes and lysosomes in rat hepatoma cells (Raposo et al., 1999) and with tubulovesicular structures in cell bodies of cultured rat superior cervical ganglion nerve cells (Lewis and Bridgman, 1996).

We investigated the function of unconventional myosins in the eukaryotic model system *D. discoideum*, a genetically tractable organism perfectly suited for the investigation of cytoskeleton-related processes in the endocytic pathway (Maniak, 1999; Neuhaus and Soldati, 1999). Our findings, obtained by a combination of molecular genetics, cell surface labeling, biochemical fractionation, and a variety of microscopy techniques, demonstrate the involvement of MyoB in the recycling of plasma membrane components from an endosomal compartment back to the cell surface. We propose that actin and MyoB are involved in the sorting of membrane from bulk fluid phase by working as mechanical support to shape the endosomal compartment and/or to help in the production of transport intermediates.

Materials and Methods

Cell Culture

D. discoideum cells of wild-type strain AX-2, *myoA*$^-$ (Titus et al., 1993), *myoB*$^-$, and *myoA*$^-$/*B*$^-$ cells (Novak et al., 1995) were grown axenically in HL5c medium (Sussman, 1987) on plastic dishes at 22°C. *myoA*$^-$/*B*$^-$ cells (Novak et al., 1995) were maintained with 10 μg/ml G418 (Calbiochem).

Antibodies

The following primary antibodies were used: (a) an mAb against the plasma membrane marker 4C4 (PM4C4)[1] called mAb V4C4F3 (Schwarz et al., 2000), a gift from Dr. J. Garin (CEA, Grenoble, France). This plasma membrane marker has not been molecularly identified, but magnetic fractionation showed that it is present throughout the endolysosomal system (Garin, J., personal communication); (b) a pAb against MyoB (Novak and Titus, 1997), a gift from Dr. M. Titus (University of Minnesota, Minneapolis, MN); (c) a pAb against MyoC, a gift from Dr. G. Côté (Queens University, Kingston, Canada); (d) an mAb against myosin II (Pagh et al., 1984), a gift from Dr. G. Gerisch (Max-Planck-Institute for Biochemistry, Martinsried, Germany); (e) a pAb against biotin (Rockland); (f) an mAb 190-340-8 against comitin, an actin binding protein shown to be a component of the Golgi apparatus, from *D. discoideum* (Weiner et al., 1993), a gift from Dr. A. Noegel (University of Köln, Köln, Germany); (g) an mAb 221-135-1 against *D. discoideum* protein disulfide isomerase (PDI), an ER resident enzyme (Monnat et al., 1997); (h) an mAb 221-35-2 against the A subunit of the vacuolar H^+-ATPase (Neuhaus et al., 1998); (i) an mAb 176-3-6 against coronin, an actin binding protein (de Hostos et al., 1993), a gift from (Dr. G. Gerisch). The secondary antibodies were either goat anti–mouse or goat anti–rabbit IgGs conjugated to Cyanine 3.29-OSu (Cy3; Rockland) or to Alexa488 (Molecular Probes).

Immunofluorescence Microscopy

Cells were plated on coverslips grade 0 (80–100 μm thick; Menzel Gläser) and allowed to adhere for several hours without selection before investigation. Pharmacologically treated cells were incubated with 10 μM cytochalasin A (cytA; Sigma-Aldrich) or 50 mM butanedione monoxime (BDM; Sigma-Aldrich) in HL5c for 15 min before freezing. The coverslips were plunged in methanol at −85°C, and then, using a homemade Dewar-based temperature-controlled apparatus, they were warmed to −35°C. Next, they were plunged in PBS at room temperature, and incubated with PBS containing 0.2% gelatin (Neuhaus et al., 1998). After staining, samples were mounted in ProLong Anti-Fade medium (Molecular Probes). Mounted samples were investigated with a Leica confocal microscope DM/IRB using a 63× objective with NA 1.4. Confocal optical sections were recorded at 0.4 μm per vertical step and eight times averaging; image stacks were imported into Adobe Photoshop® (Adobe Systems Inc.) for image processing or Image Gauge v3.0 (Fuji Film) for quantitation.

Rapid Freezing of Cell Monolayers

Cells were prepared as described by Neuhaus et al. (1998) by plating on thin sapphire coverslips (Groh+Ripp) and plunged into a liquid ethane slush at −175°C using a guillotine-like device. Samples were freeze-substituted, infiltrated with Lowicryl HM-20 (Bioproducts SERVA), and polymerized at −45°C under UV light. Sections of 100-nm thickness (silver/light gold interference color) were cut horizontally to the plane of the coverslip and placed onto Formvar carbon–coated 100 mesh hexagonal copper grids. Sections were poststained for 10 min with 4% osmium tetroxide and lead citrate.

Uptake Experiments

D. discoideum cells were plated on coverslips and incubated with HL5c medium containing fluid phase markers either for immunofluorescence or electron microscopical experiments. Yellow-green fluorescent nanobeads

[1]*Abbreviations used in this paper:* BDM, butanedione monoxime; cytA, cytochalasin A; MESNA, mercaptoethane sulfonic acid; PM4C4, plasma membrane marker 4C4; PDI, protein disulfide isomerase; SBS, Soerensen buffer containing sorbitol.

(FluoSpheres, diameter 20 nm; Molecular Probes) were used as the fluid phase marker for light microscopical investigations, as they turned out to be much better retained after methanol fixation than other available marker molecules such as lucifer-yellow, labeled dextran, and labeled proteins. 14-nm colloidal gold particles, prepared according to Slot and Geuze (1985), complexed with bovine serum albumin (BSA), as described by Griffiths (1993), were used to label endosomes for electron microscopical investigations. To follow membrane uptake, *D. discoideum* cells were washed with prechilled SBS (Soerensen buffer, 14.7 mM KH_2PO_4 and 2 mM Na_2HPO_4, with 120 mM sorbitol), pH 7.8, and incubated with ice-cold SBS, pH 7.8 containing 2 mg/ml sulfo-NHS-biotin for 30 min at 0°C. Afterwards, excess biotin was quenched by addition of SBS containing 100 mM glycine, and cells were washed with SBS again, resuspended in HL5c medium, and allowed to adhere to coverslips at 22°C to permit trafficking of biotinylated plasma membrane proteins. The cells were then processed as described for the different microscopical techniques.

To visualize acidic compartments, adherent *D. discoideum* cells were incubated with LysoSensor Green DND-189 (an acidotropic probe that may localize in the membrane of acidic organelles; Molecular Probes Product information sheet) for 5 min, washed in SBS, and imaged with a Zeiss Axiophot 2 microscope using a 100× Achroplan water immersion objective. Pictures were taken with a CCD camera (Imago Sensicam; Till Photonics).

Recycling Assay

Biotinylation of cell surface proteins was performed using a modified version of the assay of Bacon and coworkers (1994). 5×10^6 *D. discoideum* cells plated on 6-cm plastic dishes were washed once with prechilled SBS, pH 7.8, and incubated with 1 ml ice-cold SBS, pH 7.8, containing 1 mg/ml sulfo-NHS-SS-biotin (Pierce Chemical Co.) for 10 min on an ice bath. Biotinylation was stopped by washing the cells with ice-cold SBS, followed by ice-cold quenching buffer (SBS containing 100 mM glycine). Cells were then incubated with HL5c medium at 22°C for 5 min to allow internalization of biotinylated plasma membrane proteins. Uptake was stopped by placing the cells on ice and washing them with ice-cold SBS. Biotin was cleaved off of exposed surface components by incubating the cells with 100 mM of the membrane impermeant reducing agent mercaptoethane sulfonic acid (MESNA; Sigma-Aldrich) in SBS, pH 8.2, for 12 min. When cells were kept at 0°C to prevent internalization of biotinylated plasma membrane, this treatment quantitatively stripped all biotin. After stripping, cells were again washed and incubated with HL5c medium at 22°C to allow further trafficking of internalized, labeled membranes. At indicated time points, this incubation was again stopped by washing the cells with ice-cold SBS. Biotin that had been reexposed at the plasma membrane was cleaved off by incubation with MESNA for 12 min. Finally, the cells were washed with ice-cold SBS, collected from the dish with 15 ml SBS, and centrifuged for 2 min at 500 *g*. The cell pellet was resuspended once in ice-cold Soerensen buffer, centrifuged, lysed in nonreducing sample buffer (30% glycerol, 3% SDS, 125 mM Tris-Cl, pH 6.8), and boiled at 95°C for 3 min. 10^6 cells were loaded per lane of 7.5% SDS-PAGE gels, transferred to nitrocellulose membrane (Protran; Schleicher & Schuell), and stained with Ponceau S (Sigma-Aldrich). The nitrocellulose membranes were blocked with TBS (150 mM NaCl, 50 mM Tris-Cl, pH 7.4) containing 3% nonfat dried milk (Carnation) and incubated with streptavidin–HRP diluted in 5% BSA (Sigma-Aldrich) in TBS. Detection was performed with ECL plus (Amersham Pharmacia Biotech) using a chemiluminescence imager (Las-1000; Fuji Film). Data quantification was carried out with Image Gauge v3.0 (Fuji Film).

Magnetic Fractionation of Early Endosomes

Magnetic fractionation of early endosomes was performed (Adessi et al., 1995) by feeding the cells with dextran-coated iron oxide for 15 min, lysing the cells, and isolating the iron-containing endosomes from the postnuclear supernatant on a steel wool-containing column placed in a magnetic field. The endosomes were eluted, pelleted, and lysed in sample buffer (30% glycerol, 3% SDS, 125 mM Tris-Cl, pH 6.8, 100 mM DTT). Then, they were run on an 8% SDS-PAGE gel and transferred to nitrocellulose membrane (Protran; Schleicher & Schuell). For the ATP-release experiment, a pellet of isolated endosomes was resuspended in buffer containing 25 mM ATP, incubated for 5 min at 20°C, and centrifuged. Equivalent amounts of both fractions, supernatants and pellets, were lysed in sample buffer, run on SDS-PAGE gels, and transferred to nitrocellulose membranes. After blocking, membranes were incubated with primary anti-MyoB, -MyoC, and –myosin II antibodies diluted in 3% milk/TBS, washed, and incubated with secondary anti–rabbit antibodies conjugated to HRP diluted in 3% milk/TBS.

Results

Steady State Distribution of a Plasma Membrane Marker in Myosin I–deficient Cells

Immunofluorescence analysis of different myosin I–deficient cells showed a striking redistribution of the plasma membrane marker PM4C4, as revealed by antibody staining (Fig. 1). In wild-type cells (Fig. 1, wt) it mainly localized to the plasma membrane and, as the membrane is taken up via endocytosis, to intracellular vacuoles. Labeling intensities on these intracellular vacuoles were weaker than at the plasma membrane, perhaps reflecting the fact that efficient and early recycling of plasma membrane components were taking place. In *myoA/B*-deficient cells at steady state, this marker was redistributed to endosomal vacuoles; it was found to a lesser extent at the plasma membrane than on intracellular vacuoles (Fig. 1, *A-B-*). Compared with wild-type cells, the PM4C4-positive vacuoles of *myoA/B* null cells were more homogenous in size. The altered distribution of PM4C4 likely primarily arose from the absence of MyoB, as *myoB* single mutants (Fig. 1, *B-*), but not *myoA* single mutants (Fig. 1 *A-*) showed a phenotype similar (but not identical) to the double mutant cells. Nevertheless, as the effect was slightly more pronounced in *myoA/B* null cells and because strains with multiple, but not single myosin gene deletions have been reported to show endocytosis defects (Novak et al., 1995; Jung et al., 1996), the *myoA/B* null cells were further investigated.

The redistribution of PM4C4 did not result from a general disturbance of the cytoskeleton, but, more likely, from an impairment of myosin function. Indeed, the staining pattern observed after incubation with the F-actin depolymerizing agent cytA was close to the wild-type labeling pattern (Fig. 1, cytA). In sharp contrast, short treatment of wild-type cells with BDM, a general inhibitor of myosin ATPases, resulted in a redistribution of PM4C4 to intracellular structures (Fig. 1, BDM), similar to what was observed for the $myoA^-/B^-$ and $myoB^-$ cells.

To quantify this effect, the ratio of labeling intensities at the plasma membrane and on endosomes was measured in confocal sections. Therefore, line scans were performed through several wild-type and $myoA^-/B^-$ cells, the mean intensity values on the plasma membrane and on intracellular structures were determined, and the ratio of plasma membrane to endosomes per line scan was calculated as shown (Fig. 2). Evaluation of 78 line scans through wild-type and 53 line scans through myosin-deficient cells resulted in plasma membrane to endosome ratios of 2.8 ± 1.43 and 0.34 ± 0.25, repectively. This eightfold concentration of PM4C4 on endosomal vacuoles might be explained by an anomalous flux of membrane components through the endosomal compartments.

PM4C4-positive Compartments Belong to the Endolysosomal System

To verify that the PM4C4-labeled vacuoles indeed belong

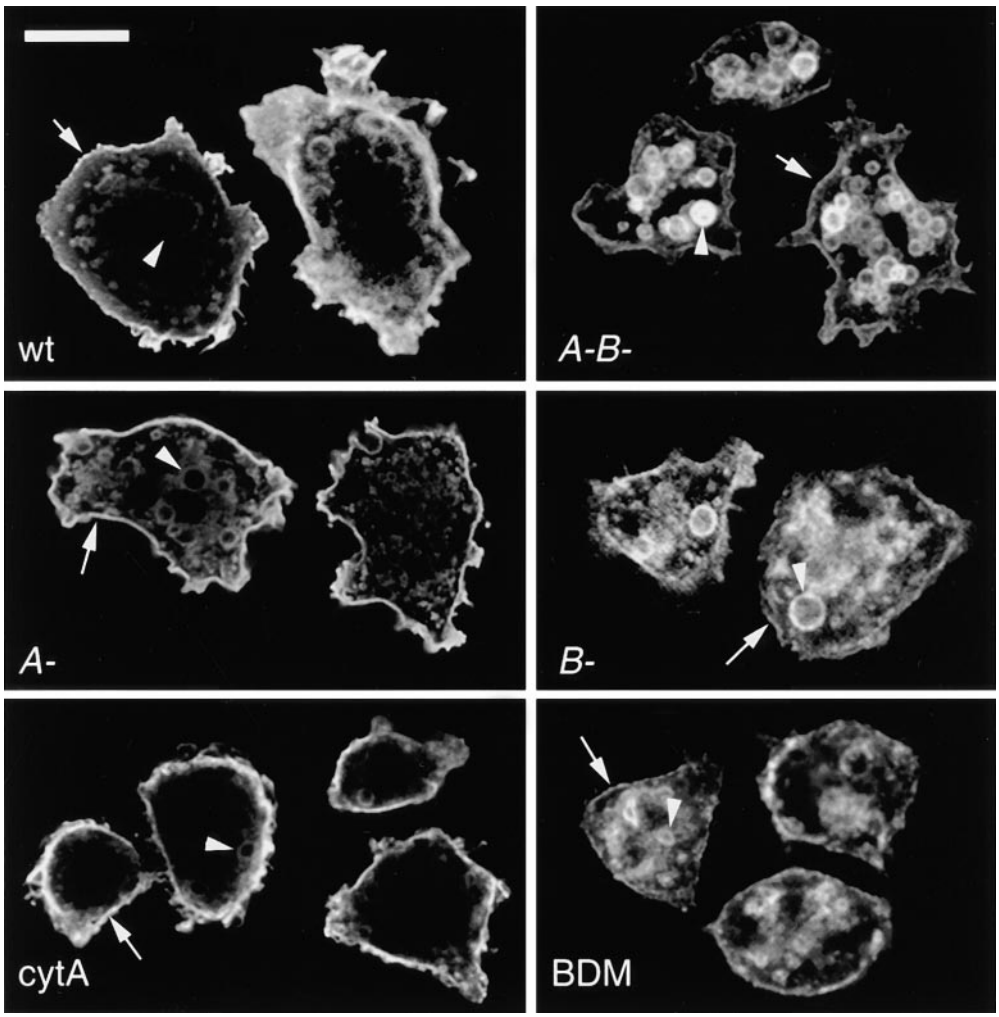

Figure 1. Distribution of a plasma membrane marker. An antibody directed against the plasma membrane marker PM4C4 strongly labeled the plasma membrane (arrows) and to a lesser extent intracellular endosomal vacuoles (arrowheads) in wild-type *D. discoideum* cells (wt). *myoA*$^-$/*B*$^-$ (*A-B-*) cells displayed higher labeling intensities on intracellular endosomal vacuoles than at the plasma membrane. *myoA*$^-$ cells (*A-*) and cytA-treated wild-type cells (cytA) showed a staining pattern resembling the wild-type situation. *myoB*$^-$ cells (*B-*) and BDM-treated wild-type cells (BDM) looked similar to *myoA*$^-$/*B*$^-$ cells. Single confocal sections. Bar, 10 μm.

to the endolysosomal system, the fate of endocytosis markers was followed (Fig. 3). Fluid phase uptake was visualized by feeding cells with fluorescently labeled nanobeads of 20-nm size (Fig. 3, a and c, nanobeads). Among the many fluid phase markers tested, the nanobeads appeared best suited for live microscopy and for optimal retention during the methanol fixation procedure. The concentration of internalized marker varied from endosome to endosome, in fixed and live cells, and was likely a function of their degree of maturation (Neuhaus, E.M., and T. Soldati, manuscript in preparation). In Fig. 3, a and c, arrows and arrowheads point to vacuoles with low and high concentrations of nanobeads, respectively. After 90 min of feeding, each PM4C4-positive compartment, in wild-type as well as in *myoA*$^-$/*B*$^-$ cells, contained detectable amounts of the fluid phase marker, demonstrating their belonging to the endosomal system (Fig. 3, a and c, PM4C4 and overlay).

In addition to this colocalization of PM4C4 with ingested fluid phase marker, we investigated whether internalized membrane proteins have access to the compartments that accumulate PM4C4 (Fig. 3, b and d). First, plasma membrane proteins were labeled at 0°C with a biotin-conjugated cross-linker. Then, before fixation, the cells were incubated in medium at 22°C to allow trafficking of biotinylated proteins. Internalized plasma membrane proteins (Fig. 3, b and d, biotin) colocalized with each of the PM4C4-labeled structure in wild-type and *myoA*$^-$/*B*$^-$ cells (Fig. 3, b and d, PM4C4 and overlay). In addition, *myoA*$^-$/*B*$^-$ cells accumulated higher concentrations of biotinylated plasma membrane proteins on intracellular PM4C4-positive vacuoles than wild-type cells (Fig. 3, b and d, PM4C4). The relative intensities of biotin and PM4C4 labeling on intracellular vacuoles did not always correspond to each other: some vacuoles had higher intensities of the biotin labeling (Fig. 3, b and d, arrows) and others had higher intensities of PM4C4 labeling (Fig. 3, b and d, arrowheads).

It is unlikely that the vacuoles accumulating PM4C4 belong to the contractile vacuole, the other prominent endomembrane system in *D. discoideum*, as staining of myosin-deficient cells for the contractile vacuole markers vacuolar H^+-ATPase (Fig. 4 a, v-H^+-ATPase) and calmodulin (data not shown) did not differ from the wild-type staining patterns. Moreover, the morphology of other endomembrane compartments was undisturbed and the constitutive secretory pathway was not altered in the mutant cells (Temesvari et al., 1996). The PM4C4-positive vacuoles in *myoA*$^-$/*B*$^-$ cells did not stem from anomalous ER or Golgi cisternae, as staining for the ER resident enzyme

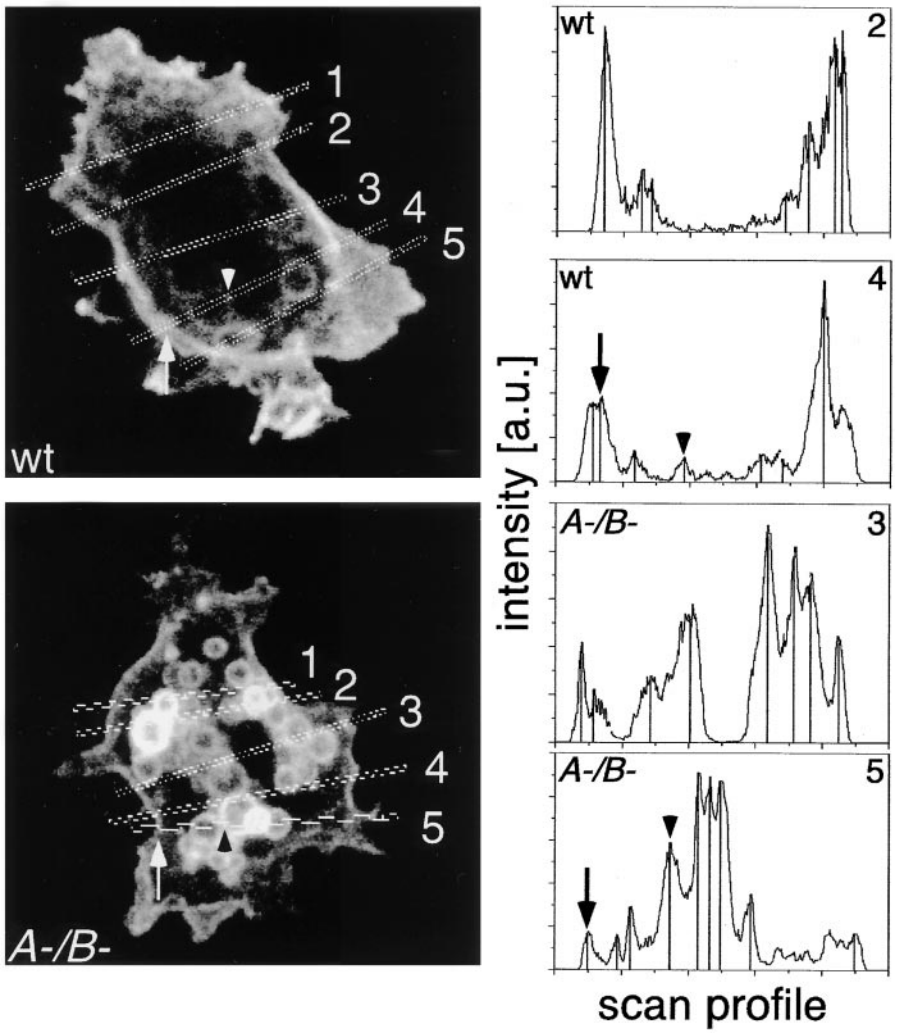

Figure 2. Quantification of the membrane concentration of the marker PM4C4. The steady state concentration of PM4C4 on the cell surface (arrows) compared with endomembranes (arrowheads) of wild-type (wt) and *myoA/B* mutant cells *A-/B-* was determined. Representative confocal sections of both cell types with two examples of scan profiles are shown. Peaks corresponding to plasma membrane (arrows) and endosomes (arrowheads) are marked as in the corresponding confocal section. Analysis of peak intensities of 78 line scans through wild-type cells and 53 line scans through *myoA⁻/B⁻* cells resulted in ratios of plasma membrane versus endosomal membranes stainings of 2.80 ± 1.43 for wild-type and 0.34 ± 0.25 for *myoA⁻/B⁻* cells.

PDI (Fig. 4 a) and for comitin (Fig. 4 a, comitin), an actin-binding protein associated with the Golgi apparatus, did not differ from the wild-type.

Endosomes in myoA⁻/B⁻ Cells Are Acidic

In *D. discoideum*, it has been shown that as early as 1–2 min after ingestion and release of the cytoskeletal coat consisting of actin and coronin (Maniak et al., 1995), the endosomal pH drops significantly (Maniak, 1999), reaches a minimum at ~15 min, and slowly rises afterwards (Aubry et al., 1993; Padh et al., 1993). No significant change was detected in the number of intracellular coronin-positive vacuoles in *myoA⁻/B⁻* cells, indicating that the macropinosomes likely shed their cytoskeletal coat at normal rates (Fig. 4 b, coronin). Acidic compartments can be visualized in live cells by the pH-sensing reagent LysoSensor, a membrane-permeant weak base that is trapped in acidic compartments upon protonation and shows a pH-dependent increase in fluorescence. Wild-type and *myoA⁻/B⁻* cells were incubated with LysoSensor Green (Fig. 4 b, lysosensor). Whereas in wild-type cells labeled compartments exhibited a large size variation, they were relatively big and homogenous in size in *myoA⁻/B⁻* cells. The uniform morphology, the size, and the high abundance of these acidic vacuoles suggest that they are identical to the compartment accumulating PM4C4.

Membrane Recycling Is Defective in Myosin Mutants

The observed concentration of PM4C4 on endosomal vacuoles in *myoA⁻/B⁻* cells might be explained by a membrane recycling defect. To directly test this hypothesis, we adapted a protocol primarily used to monitor membrane uptake and based on reversible biotinylation of plasma membrane proteins (Bacon et al., 1994; Novak et al., 1995; and illustrated in Fig. 5 a). Control experiments for each of the multiple steps of this recycling assay are shown in Fig. 5 b.

Plasma membrane proteins were biotinylated in adherent *D. discoideum* cells at 0°C with a biotin-conjugated cross-linker containing a disulfide bridge. Western blotting of *D. discoideum* cell extracts with streptavidin-HRP before and after biotinylation (control lane and +biotin lane, respectively, in Fig. 5 b, biotinylation) showed a prominent band at ~80 kD corresponding to an endogenous biotin-containing protein. The major band resulting from biotinylation appeared at ~120 kD and corresponds to gp126, a

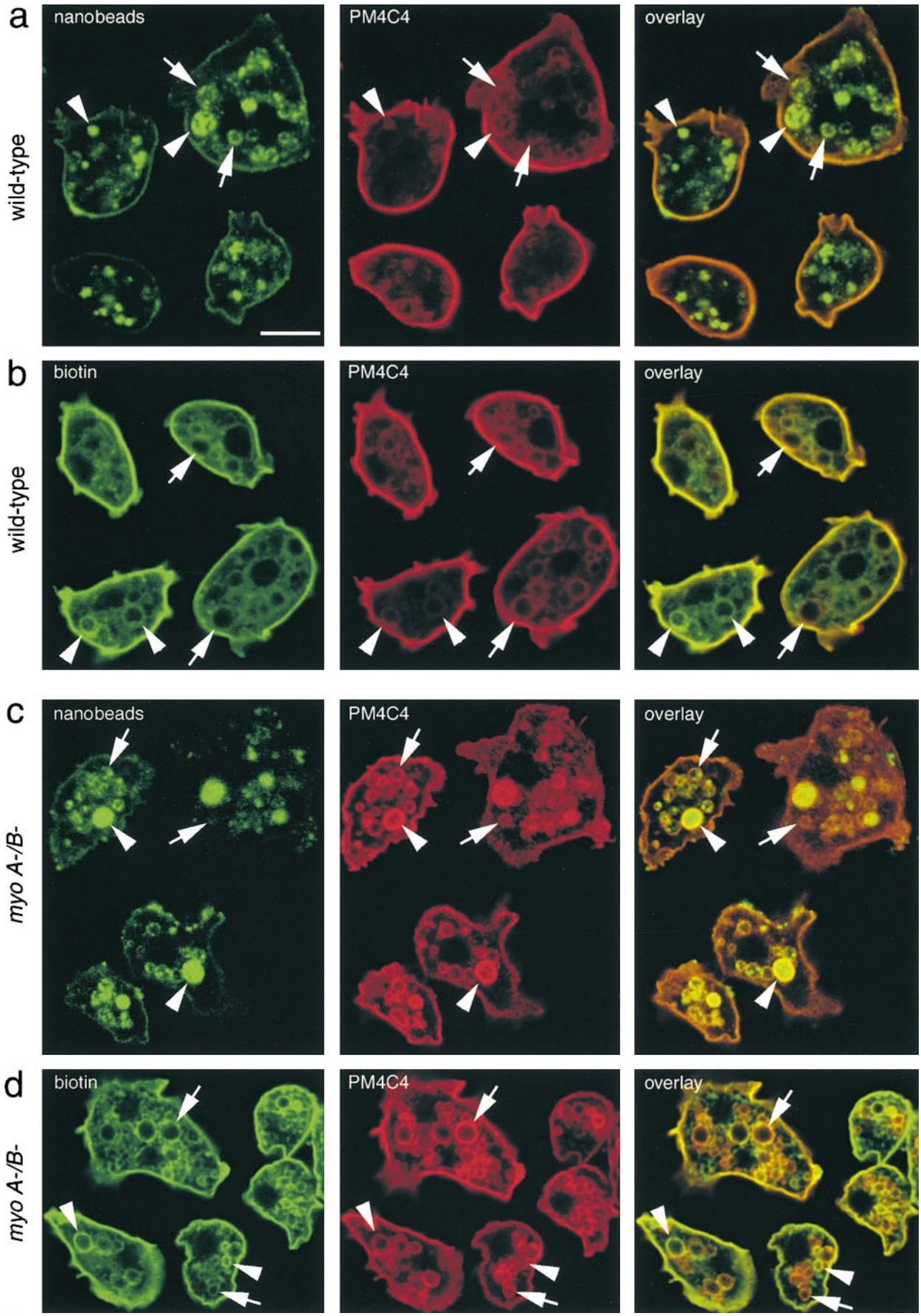
a
nanobeads
PM4C4
overlay
wild-type
b
biotin
PM4C4
overlay
wild-type
c
nanobeads
PM4C4
overlay
myo A-/B-
d
biotin
PM4C4
overlay
myo A-/B-

cell surface protein that is internalized at room temperature (Bacon et al., 1994). This signal disappeared after biotin was cleaved off with the membrane-impermeant reducing agent MESNA (Fig. 5 b, biotinylation).

After uptake of labeled plasma membrane into endosomes (Fig. 5 a, uptake), internalized biotin should become inaccessible to cleavage by MESNA (Fig. 5 a, cleavage 1). As expected, increasing amounts of biotinylated 120-kD protein became inaccessible to cleavage by MESNA with time (+MESNA lanes in Fig. 5 b, uptake wt). Note that the total amount of biotin incorporated in the samples (−MESNA lanes in Fig. 5 b, uptake wt) remained constant, excluding that the 120-kD labeled protein was significantly degraded during the experiment. Similarly, in *myoA*$^-$/*B*$^-$ cells a portion of the biotinylated marker protein was internalized and became resistant to MESNA cleavage (Fig. 5 b, uptake *myoA*$^-$/*B*$^-$). The membrane uptake rates estimated from the first time points of these experiments revealed that internalization of one cell surface equivalent occurs every 18 ± 4 min in wild-type cells and every 28 ± 4 min in *myoA*$^-$/*B*$^-$ cells. These data confirm quantitatively the earlier qualitative observation (Novak et al., 1995) that *myoA*$^-$/*B*$^-$ cells internalize membrane components slower than wild-type cells. As the rates of fluid phase uptake were similar in the two strains (data not shown), the reason for this decrease could reside in a difference in the average size of the primary pinosomes, but was not further investigated in the present study.

After a 5-min uptake pulse followed by MESNA cleavage at 0°C, further trafficking of biotinylated membrane proteins was allowed at 22°C (Fig. 5 a, chase). The total amount of endocytosed biotinylated 120-kD protein (cleavage 1 resistant) remained constant over the duration of the experiment (Fig. 5 b, chase wt), demonstrating that neither was it degraded, nor was the biotin cleaved off during passage in the endolysosomes.

If the 120-kD proteins become reexposed at the plasma membrane, they are again accessible to MESNA cleavage at 0°C (Fig. 5 a, cleavage 2) and only the biotin remaining protected in intracellular compartments is detected by Western blotting. In wild-type cells, the intensity of the intracellular, cleavage 2–resistant 120-kD band continuously decreased with increasing time of chase at 22°C (Fig. 5 c, wt), demonstrating for the first time that early membrane recycling occurs in *D. discoideum*. In sharp contrast, except for the decrease detected in the first 5 min, in *myoA*$^-$/*B*$^-$ cells the 120-kD signal remained constant for >40 min (Fig. 5 c, *A-/B-*). The intensity profiles of the 120-kD band from at least three independent experiments for each time point and cell line were quantified and the resulting curves were plotted (Fig. 5 d). Due to the difference in membrane internalization rates between both cell lines, the starting points of the recycling experiments were normalized to the amount of biotin taken up by the cells after 5 min. Wild-type *D. discoideum* cells recycled ~90% of a 5-min pulse of biotinylated plasma membrane proteins in 30–40 min, and >40–50% of the signal was recycled in the first 5 min. In *myoA/B*-deficient cells, only 30–40% of a 5-min pulse of biotinylated plasma membrane proteins was recycled after 40 min, most of it in the first 5 min. Compared with wild-type cells, the intensity of the intracellular signal in *myoA*$^-$/*B*$^-$ cells did not significantly diminish, a strong indication of a severe defect in membrane recycling from the endosomes to the cell surface.

MyoB Is Present on Early Endosomes

The presence of MyoB on early endosomes was investigated. *D. discoideum* cells were fed with colloidal iron for 15 min, and the iron-containing endosomes were magnetically purified (see Materials and Methods for details). This method has been extensively used in *D. discoideum* (Rodriguez-Paris et al., 1993; Nolta et al., 1994; Temesvari et al., 1994; Adessi et al., 1995; Souza et al., 1997) and results in a high enrichment for endolysosomal markers with very low contamination of nonendocytic organelles (plasma membrane, mitochondria, and ER are all <1%). The early endosomal proteins recovered by this procedure represented ~1% of the total amount of protein in the starting material or 2% of the particulate fraction of the postnuclear supernatant, as this fraction contains 50% of the total cell protein (data not shown).

MyoB was present in the early endosomal fraction, whereas MyoC, a closely related myosin I used as a control, was not detected in this fraction (Fig. 6 a). About 1% of total cellular MyoB was found in the early endosomal fraction. But, since 90% of total MyoB is present in a large cytosolic pool of inactive myosins, and only 10% is present in the particulate fraction of the cell lysate, this means that 10% of the MyoB present on the particulate fraction is on early endosomes. As early endosomal proteins form only 2% of the particulate fraction, this represents at least a fivefold enrichment of MyoB on the early endosomes.

The nature of the association of MyoB with the early endosomes was further examined. In the absence of ATP, myosins bind to actin filaments via their motor domain (*rigor mortis*), and this binding can be released by addition of ATP. Furthermore, myosins can bind cargos via their tail domain, which is the most variable part of the molecule and has been suggested to reflect the adaptation of myosins to specific functions (Mermall et al., 1998). In MyoB, as in many class I myosins, the tail is composed of

Figure 3. Colocalization of endocytic markers with PM4C4-positive vacuoles. (a and c) Intracellular PM4C4-positive vacuoles (PM4C4) contained endocytosed yellow-green fluorescent nanobeads as fluid phase marker (nanobeads) in both wild-type (a) and *myoA*$^-$/*B*$^-$ cells (c). Some of the PM4C4 vacuoles contained high concentrations of fluid phase marker (a and c, arrowheads); others contained only low concentrations (a and c, arrows). (b and d) The PM4C4 vacuoles also contained plasma membrane proteins that had been biotinylated at 0°C and internalized via endocytosis after warming to 22°C (biotin) in wild-type (b) and in *myoA*$^-$/*B*$^-$ cells (d). The relative labeling intensities of the vacuoles varied between both channels. Some vacuoles contained higher biotin signals (b and d, arrowheads) and appeared green in the overlay, whereas others contained higher PM4C4 signals (b and d, arrows) and appeared red in the overlay. Altogether, *myoA*$^-$/*B*$^-$ cells (d, biotin) contained more biotinylated protein on internal vacuoles than wild-type cells (b, biotin), similar to what was observed for the plasma membrane marker PM4C4 (b and d). Bar, 10 μm.

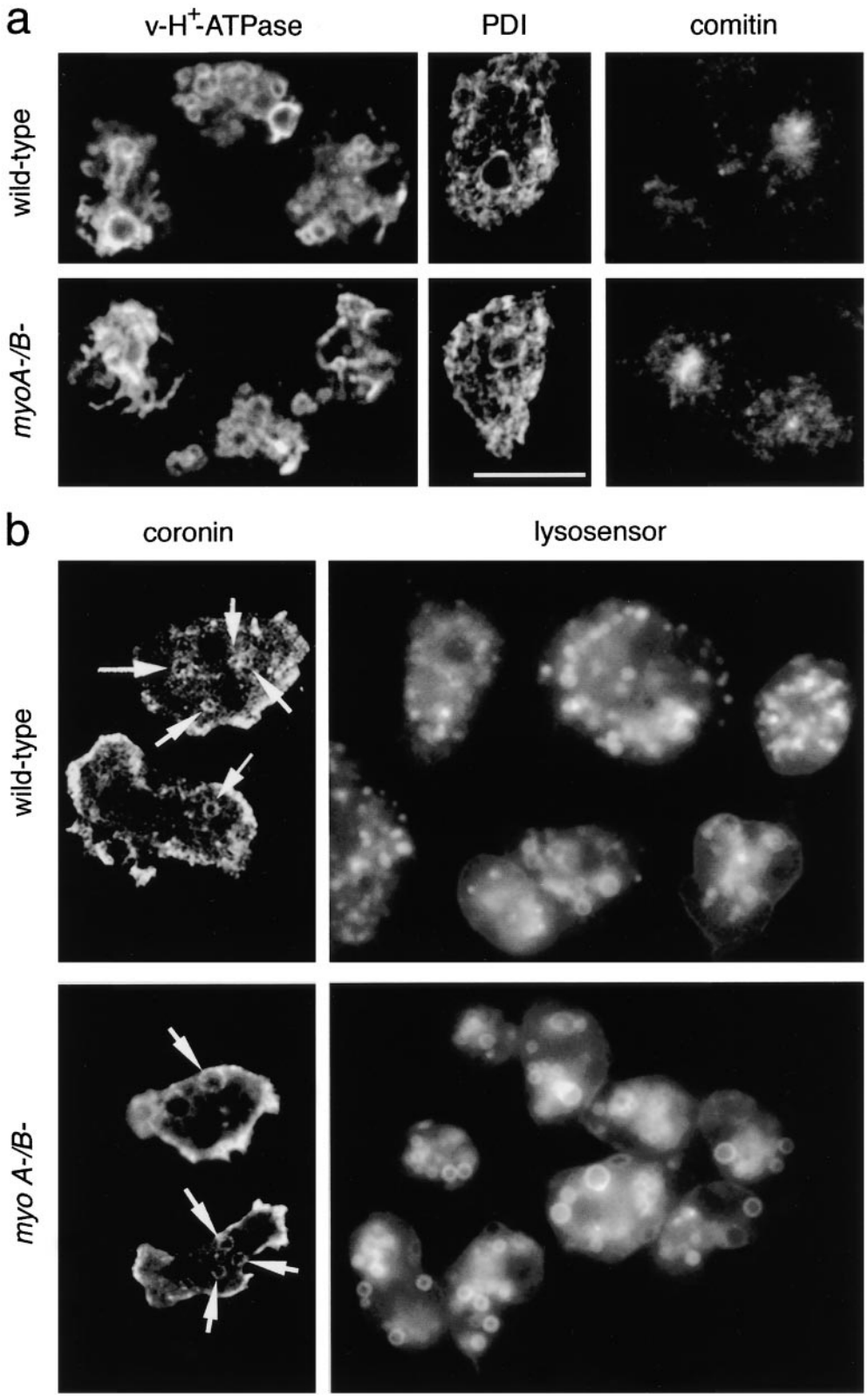

Figure 4. (a) Other major endomembrane compartments are similar in wild-type and *myoA*$^{-}$/*B*$^{-}$ cells. The contractile vacuole system was visualized with an antibody against the vacuolar H^+-ATPase (v-H^+-ATPase); the ER was labeled with an antibody against PDI; the Golgi apparatus was visualized with an antibody against the actin-binding protein comitin. (b) Endosomes in *myoA/B* null cells are acidic. *myoA*$^{-}$/*B*$^{-}$ and wild-type cells showed similar number of coronin-positive vacuoles (coronin). Staining of wild-type *D. discoideum* cells with LysoSensor Green visualized the membrane of acidic organelles with a broad size distribution (lysosensor). In *myoA*$^{-}$/*B*$^{-}$ cells, the labeled acidic compartments were more homogeneous in size. Bar, 10 μm.

three subdomains (for review see Coluccio, 1997): a basic phospholipid binding domain, a domain shown in vitro to contain a secondary ATP-independent actin-binding site, and finally, an Src homology 3 domain. To test whether MyoB is associated with the early endosomes via its motor domain or whether it is specifically associated via its tail domain, an ATP-release experiment was performed (Fig. 6 b). The small fraction of myosin II present on the endosomes served as a control. Myosin II was efficiently released from the endosomal fraction after incubation with

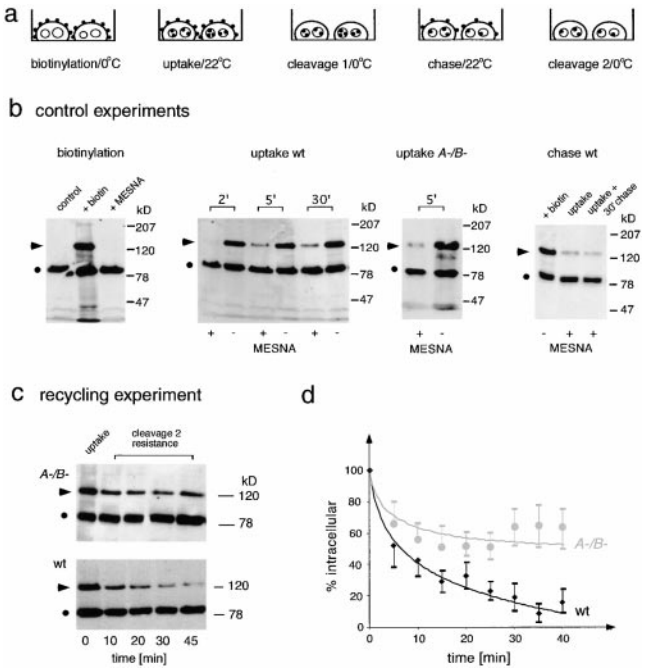

Figure 5. Establishment of a recycling assay using reversible biotinylation of plasma membrane proteins. (a) Schematic representation of the optimized recycling assay. Cell surface proteins were biotinylated (biotinylation) and internalization was allowed for 5 min (uptake). Afterwards, remaining biotin in the plasma membrane was cleaved off (cleavage 1) and further trafficking of internalized membrane was allowed (chase). Biotin was cleaved off of reexposed proteins (cleavage 2) and the remaining amount of intracellular labeling was followed over time. (b) Control experiments. Biotinylation: Western blot of *D. discoideum* cell lysates. An endogenous biotin-containing protein of 80 kD (•) was used as internal standard (first lane). After labeling of cell surface proteins at 0°C with a biotin-coupled cross-linker containing a disulfide bridge, a strong signal at 120 kD (arrowhead) and several minor bands were visible (second lane). This biotin labeling (arrowhead) could be cleaved off quantitatively by the reducing agent MESNA (third lane). Uptake wt: Due to internalization of labeled plasma membrane at 22°C, increasing amounts of the 120-kD biotin signal (arrowhead) became protected from cleavage 1 with MESNA (+MESNA lanes). The total amount of biotin in the samples before cleavage 1 (−MESNA lanes) was constant over time. Uptake A^-/B^-: *myo*A^-/B^- cells also internalized biotinylated plasma membrane proteins, and a cleavage 1 (+MESNA lane) resistant 120-kD biotin signal (arrowhead) was detected after 5 min uptake at 22°C. Chase wt: After internalization, the cleavage 1–resistant signal (arrowhead, uptake) stayed constant even after 30 min of chase (arrowhead, uptake + 30′ chase). (c) Recycling experiment. Representative Western blots from recycling experiments. After an initial uptake of biotinylated plasma membrane proteins (first lane, uptake) the cleavage 2–resistant 120-kD signal (arrowhead) decreased with increasing duration of chase (recycling) in wild-type cells. In contrast, in *myo*A^-/B^- cells the internalized 120-kD signal (arrowhead) stayed constant from 10 min on. (d) Quantification. Curves resulting from quantification of Western blots from three to five independent recycling experiments carried out as described in c. Wild-type cells are represented by black diamonds and *myo*A^-/B^- cells by gray circles. Error bars represent the SEM.

ATP and was detected in the supernatant (Fig. 6 b, ATP-release), indicating that it was bound via its head domain to endosome-associated actin filaments. MyoB was not released from the endosomes by incubation with ATP, indicating that binding was likely mediated by its tail domain. The tail domain could either bind to endosome-associated actin filaments via the ATP-insensitive actin-binding site or directly to the endosomal membrane via the membrane-binding site (Fig. 6 c). The specific binding of MyoB to biochemically purified early endosomes via its tail domain may be indicative of a direct involvement in the recycling of membrane components from this compartment.

Ultrastructure of Intracellular Vacuoles in myoA^-/B^- *Cells*

To determine the precise place and mode of action of MyoB, the ultrastructure of endocytic vacuoles in myosin I–deficient cells was investigated (Fig. 7). Wild-type and *myo*A^-/B^- cells were fed with BSA-covered colloidal gold particles. Freshly prepared gold particles are monodispersed, but clump together after the protein coat is digested by lysosomal enzymes (Bright et al., 1997). Clumping of particles in endosomal compartments can therefore be used as a marker for the different stages of maturation/degradation. Early endosomal vacuoles have intermediate electron density and contain only few gold particles. Concentration of the fluid phase during maturation of the endosomes results in a more electron-dense appearance of the endosomal lumen and in the accumulation of clumped gold particles. Particles also appear in compartments that have vesicular membranes in their lumen (Neuhaus, E.M., and T. Soldati, manuscript in preparation).

Rapidly frozen wild-type cells commonly exhibited one small (~110–120 nm) vesicle per 100-nm section of micrometer-sized early endosomal vacuole (Fig. 7 a, wild-type), suggesting that the whole vacuole was surrounded by <10 small vesicles. In myosin-deficient *D. discoideum* cells (Fig. 7 a, *myoA-/B-*), on average ~6 small vesicles were found around early endosomal vacuoles, suggesting that the vacuoles were surrounded by 50–100 vesicles.

Other endomembrane compartments did not show an accumulation of small vesicles (Fig. 7 b). Later endosomal vacuoles containing big aggregates of gold particles (Fig. 7 b, arrowheads) and/or membranous structures in their lumen (Fig. 7 b, arrows) were not surrounded by small vesicles, either in wild-type or in *myo*A^-/B^- cells. Also the newly formed macropinosomes, identified by their actin coat, were not surrounded by small vesicles in *myo*A^-/B^- cells (Fig. 7 b, MP). Translucent bladders free of gold particles and closely apposed to the plasma membrane most likely belong to the contractile vacuole complex, an osmoregulatory system consisting of interconnected tubules, vacuoles, and cisternae (Heuser et al., 1993). No accumulation of vesicles was discernible around the contractile vacuoles of *myo*A^-/B^- and wild-type cells (Fig. 7 b, CV).

Many of the small vesicles in *myo*A^-/B^- cells appeared to be directly attached to the vacuoles by a tether of unidentified nature (Fig. 7, c, arrowheads, and a, *myo*A^-/B^-, small arrowheads point to a ~1-μm-long tether). Interestingly, some of the vesicles had a relatively electron-dense periphery, possibly resulting from the presence of a coat

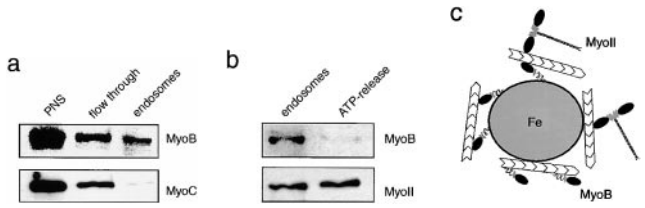

Figure 6. MyoB is found in an early endosomal fraction. (a) Wild-type *D. discoideum* cells were fed with colloidal iron for 15 min. Early endosomes were isolated by magnetic fractionation and probed for the presence of class I myosins by Western blotting using anti-MyoB and anti-MyoC antibodies. MyoB was found in the isolated endosome fraction, whereas MyoC was not significantly present. (b) ATP-release experiment. Isolated endosomes were incubated with ATP and pellets (endosomes) and supernatants (after ATP release) were analyzed by Western blotting with anti-MyoB and anti–myosin II antibodies. Myosin II was quantitatively released by ATP, most likely indicating that it was bound to endosome-attached actin filaments via its head domain. MyoB was not released, indicating that it was likely specifically bound to endosomes via its tail domain. (c) Schematic illustration of the observed binding modes.

(Fig. 7 c, arrows). It is tempting to speculate that the observed structures result from incomplete or nonproductive budding of recycling vesicles.

Discussion

Class I myosins have been implicated in endocytosis in a variety of organisms, from yeast to mammalian cells. The simple eukaryote *D. discoideum*, which is perfectly suited as a model system for the investigation of cytoskeleton-related processes in the endocytic pathway (for reviews see in Maniak, 1999; Neuhaus and Soldati, 1999), expresses seven class I myosins (Uyeda and Titus, 1997; Schwarz et al., 1999). The precise place and mode of action of these myosins are slowly being unraveled. Here, we present evidence for the function of myosin IB in the process of membrane recycling from the endosomes back to the cell surface.

MyoB in Membrane Recycling

In *D. discoideum*, significant amounts of fluid phase are taken up via macropinocytosis (Hacker et al., 1997). Therefore, the primary pinosomes are rather big vacuoles. Maturation of this primary pinocytic compartment starts immediately after release of the cytoskeletal coat and, as early as 1–2 min after ingestion, the pH drops significantly and delivery of a subset of lysosomal enzymes occurs (Aubry et al., 1993; Padh et al., 1993; Maniak, 1999). As very little or no early fluid phase recycling was observed in *D. discoideum* (Aubry et al., 1997), endocytic trafficking was proposed to be a linear process (Maniak, 1999), ending with the exocytosis of food remnants from postlysosomes (Jenne et al., 1998; our unpublished observations). But membrane components not destined for degradation have to be recycled back to the plasma membrane. Moreover, homeostasis of the size of the pinocytic compartment implies that delivery of membranes containing the proton pumps and lysosomal enzymes has to be compensated by an equally rapid and efficient retrieval of membrane. Here, we show that this indeed happens in *D. discoideum*. Membrane recycling from endosomes occurs with a complex kinetics: ~50% of a 5-min pulse of biotinylated plasma membrane proteins is recycled in 5 min, and the remaining marker reaches the cell surface in the next 30–40 min. Mammalian cells show a biphasic recycling kinetics with direct, fast recycling from the early sorting endosome and slow recycling from the recycling endosome (Ghosh et al., 1994; Sheff et al., 1999). *myoA*$^-$/*B*$^-$ cells show recycling of 30–40% of a 5-min uptake pulse in the first 5 min, but show no further recycling in the next hour. As a result of this defect, *myoA*$^-$/*B*$^-$ cells accumulate the plasma membrane marker PM4C4 on intracellular endocytic vacuoles. As *myoB*$^-$, but not *myoA*$^-$ cells accumulate this marker in a very similar manner, we conclude that MyoB might be responsible for membrane recyling in *D. discoideum*. Interestingly, there is recent evidence that class I myosins play a role in endocytic membrane trafficking along the recycling pathway in polarized epithelial cells (Durrbach et al., 2000; Huber et al., 2000).

Molecular Function of MyoB in the Maintenance of Endosome Morphology

An increased number of small vesicles was found in the immediate vicinity of early endocytic vacuoles in *myoA*$^-$/*B*$^-$ cells. Many of these vesicles were tethered to the vacuole surface. Some of these vesicles have a relatively electron-dense periphery, suggesting the presence of a coat. Clathrin-coated vesicles have been involved in the recycling process in mammalian cells (Stoorvogel et al., 1996; Futter et al., 1998). A close relationship between clathrin-coated

Figure 7. (a) Ultrastructure of early endocytic vacuoles in *myoA*$^-$/*B*$^-$ cells. Thin sections of rapidly frozen *myoA/B*-deficient *D. discoideum* cells *(myoA*$^-$/*B*$^-$*)* presented an accumulation of small (110–120 nm) vesicles (arrowheads) around big endolysosomal vacuoles containing internalized BSA-gold. These vacuoles contained only few dispersed gold particles, indicating that they were relatively early endosomes. Some of the vesicles were tethered to the vacuoles (small arrowheads). Vacuoles in wild-type cells (wild-type) did not show this accumulation of vesicles (arrowheads). (b) Ultrastructure of late endosomes and of the contractile vacuole. Later endocytic compartments containing higher concentrations of gold particles (aggregated because the BSA coat is digested by lysosomal enzymes) were identified by the presence of intralumenal membranous structures (arrows) or a relatively electron-dense content (arrowheads). Newly formed macropinosomes (MP) contained few dispersed gold particles and were surrounded by an F-actin layer. The contractile vacuole (CV) was identified by the complete absence of ingested gold particles, its characteristic shape, and direct apposition to the plasma membrane (PM). None of these structures showed an accumulation of small vesicles, neither in wild-type, nor in *myoA*$^-$/*B*$^-$ cells. (c) Higher magnification of tethered vesicles in *myoA*$^-$/*B*$^-$ cells. Some of the small vesicles accumulated around early endocytic vacuoles in *myoA*$^-$/*B*$^-$ cells had a relatively electron-dense periphery (arrows), and often seemed to be connected to the vacuole by thin tethers (arrowheads). Bars: (a and b) 1 μm; (c) 0.2 μm.

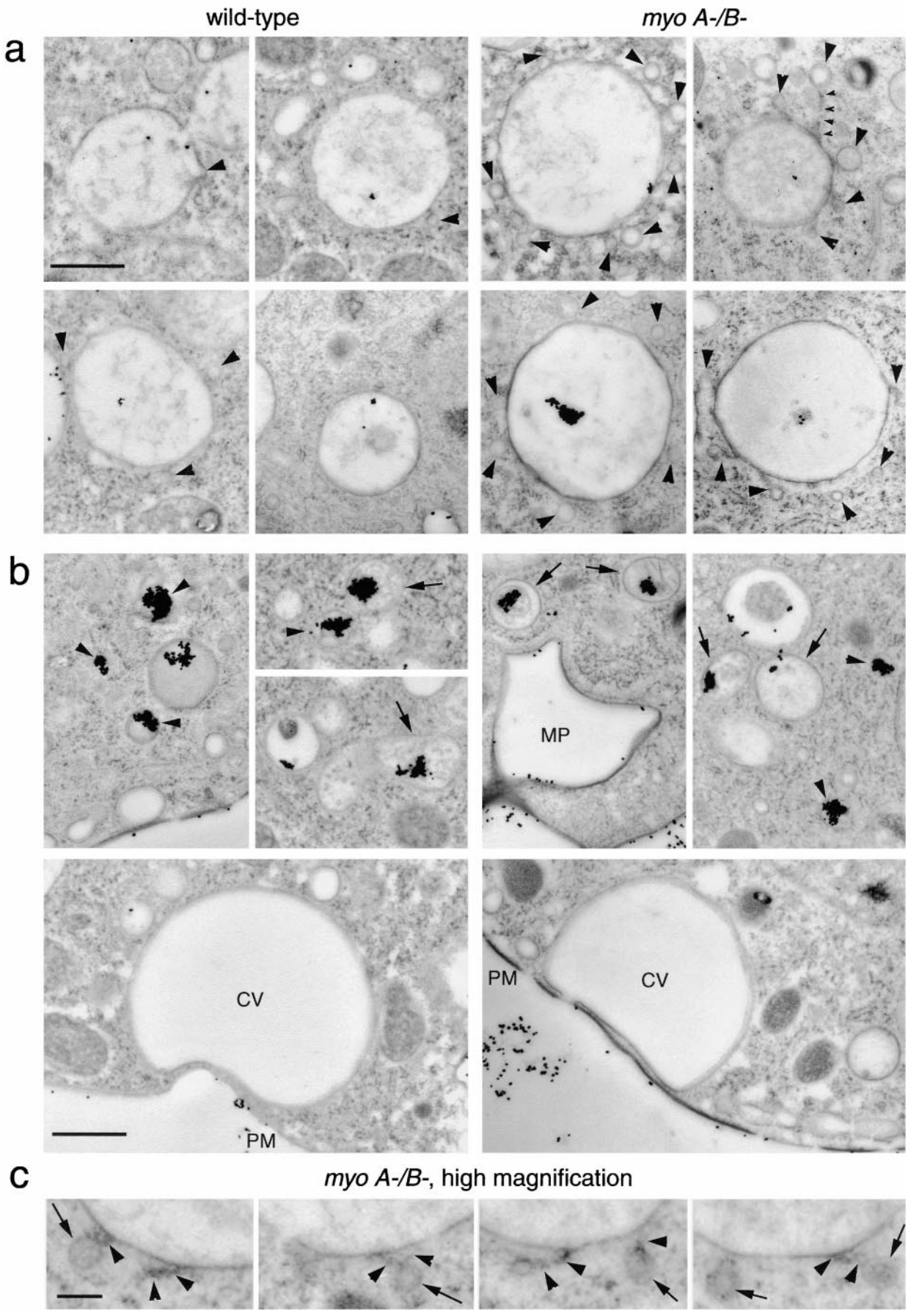
wild-type
myo A-/B-
a
b
MP
CV
PM
CV
PM
c
myo A-/B-, high magnification

vesicle formation, motility, and the actin cytoskeleton was recently shown in *D. discoideum* (Damer and O'Halloran, 2000). These findings suggest that MyoB could help maintain the proper morphology of the endosomal compartment involved in recycling, thereby enabling efficient sorting of membranes from fluid phase. One might speculate that, together with actin filaments, MyoB could be involved in the formation of a contractile ring or spiral around the vesicle neck, thereby helping it to pinch off. Alternatively, actin and MyoB could act as a coat and provide the driving force to bud off a vesicle, or it may function as a bona fide motor and transport vesicles along the actin filaments away from the donor organelle. Indeed, possible roles in the process of vesicle budding and/or scission have been discussed for the yeast MyoB homologues, Myo5p and Myo3p, that are involved in receptor-mediated endocytosis (Geli and Riezman, 1998).

Physiological Impact of MyoB Deletion

Earlier investigations demonstrated that *myoB*$^-$ cells exhibit a reduced efficiency of chemotactic aggregation and cell motility in only 51% of the of wild-type cells (Jung and Hammer, 1990; Wessels et al., 1991). The reduction in cell motility of *myoB*$^-$ cells could be a result of the impaired membrane flow from the endosomes back to the plasma membrane. Membrane flow models for cell locomotion, in which the advance of the leading edge is provided by membrane from internal pools, have been proposed (Abercrombie et al., 1970; Bretscher, 1996). The delivery of receptors to the leading edge of migrating cells (Hopkins et al., 1994; Lawson and Maxfield, 1995; Pierini et al., 2000) closely link membrane recycling and cell movement.

We estimated initial rates of membrane uptake in wild-type cells from the first time point of the biotinylation experiment and showed that internalization of one cell surface equivalent occurs every 18 ± 4 min. Using a fluorimetric assay, Aguado-Velasco and Bretscher recently measured that *D. discoideum* amebas endocytose one cell surface equivalent every 4–10 min (Aguado-Velasco and Bretscher, 1999). Earlier studies, which followed cell surface proteins labeled with radioactive galactose, reported a plasma membrane internalization rate of 45 min (Thilo and Vogel, 1980; Thilo, 1985). It was shown that *D. discoideum* cells take up fluids mainly via macropinocytosis. We calculated that formation of five macropinosomes per minute with an average diameter of 1.6 μm (Hacker et al., 1997) leads to the uptake of one cell surface equivalent every 24 min, which is in the range of our experiments. These high uptake rates may be well correlated with the elevated endocytic membrane flow necessary for rapid directed movement during chemotaxis (Aguado-Velasco and Bretscher, 1999).

More evidence for links between motility and membrane flow comes from the investigation of several mutants, for example *D. discoideum* cells lacking clathrin heavy chain or coronin (for review see Gerisch et al., 1999). The role of MyoB in membrane recycling could therefore be one factor contributing to the reported reduction in cell motility of *myoB*$^-$ cells (Jung and Hammer, 1990; Wessels et al., 1991).

Furthermore, defects in the uptake of yeast were observed in *myoA*$^-$/*B*$^-$ cells assayed on substratum (our unpublished observations), although other studies found no reduction of phagocytosis in suspension-grown *myoA*$^-$/*B*$^-$ cells (Novak et al., 1995). Phagocytosis was found to be reduced in *myoB*$^-$, but not *myoA*$^-$ cells (Jung and Hammer, 1990). These defects are interesting in light of the recent discussion emphasizing the tight mechanistic relationship between phagocytosis and cell motility (Mellman, 2000). The requirement for vectorial insertion of membrane at sites of membrane protrusions may link both processes to the accurate and polarized recycling of plasma membrane from the endosomes back to the cell surface (Bajno et al., 2000; Mellman, 2000).

Summary

The molecular mechanisms of membrane trafficking in the simple eukaryote *D. discoideum* show extensive similarities to mammalian cells (Neuhaus and Soldati, 1999). Nevertheless, the linearity of the major endosomal fluid phase flux was thought to illustrate a major discrepancy between these organisms. Here we show that *D. discoideum* cells, like mammalian cells, efficiently recycle plasma membrane components from an early endocytic compartment, indicating that major transport steps are conserved between these organisms. We further show that a myosin I is involved in this membrane recycling step. This work highlights that, besides the extensively studied signal-based sorting mechanisms, actin and myosin may be implicated in the sorting of membrane and contents. We propose that, together with the formation of specialized lipid domains (for review see Mukherjee and Maxfield, 2000), the actin–myosin cytoskeleton may build the mechanical support to shape some intracellular compartments and produce transport carriers, thereby providing the foundation for geometry-driven sorting processes.

We especially thank Dr. M. Titus for the gift of myosin-deficient cell lines, antibodies, and for lots of helpful comments, and also Dr. J. Garin for performing the magnetic fractionation experiments and for the gift of the plasma membrane marker antibody. We further thank Dr. M. Maniak (Kassel University, Kassel, Germany) for helpful discussions and donation of antibodies. Drs. G. Côté, G. Gerisch, and A. Noegel kindly provided antibodies. Thanks also to Drs. M.I. Geli, H.-H. Gerdes (both University of Heidelberg), and E. Schwarz for their helpful comments on the manuscript.

The work was supported by a grant from the Deutsche Forschungsgemeinschaft (SFB 352) and by the Max-Planck Gesellschaft (doctoral fellowship to E.M. Neuhaus).

Submitted: 2 February 2000
Revised: 10 July 2000
Accepted: 11 July 2000

References

Abercrombie, M., J.E.M. Heaysman, and S.M. Pegrum. 1970. The locomotion of fibroblasts in culture. 3. Movement of particles on the dorsal surface of the leading lamella. *Exp. Cell Res.* 62:389–398.

Adessi, C., A. Chapel, M. Vincon, T. Rabilloud, G. Klein, M. Satre, and J. Garin. 1995. Identification of major proteins associated with *Dictyostelium discoideum* endocytic vesicles. *J. Cell Sci.* 108:3331–3337.

Aguado-Velasco, C., and M. Bretscher. 1999. Circulation of plasma membrane in *Dictyostelium*. *Mol. Biol. Cell.* 10:4419–4427.

Aubry, L., G. Klein, J.L. Martiel, and M. Satre. 1993. Kinetics of endosomal pH evolution in *Dictyostelium discoideum* amoebae. Study by fluorescence spectroscopy. *J. Cell Sci.* 105:861–866.

Aubry, L., G. Klein, J.L. Martiel, and M. Satre. 1997. Fluid-phase endocytosis

in the amoebae of the cellular slime mould *Dictyostelium discoideum*: mathematical modelling of kinetics and pH evolution. *J. Theor. Biol.* 184:89–98.
Bacon, R.A., C.J. Cohen, D.A. Lewin, and I. Mellman. 1994. *Dictyostelium discoideum* mutants with temperature-sensitive defects in endocytosis. *J. Cell Biol.* 127:387–399.
Bajno, L., X.-R. Peng, A.D. Schreiber, H.-P. Moore, W.S. Trimble, and S. Grinstein. 2000. Focal exocytosis of VAMP3-containing vesicles at sites of phagosome formation. *J. Cell Biol.* 149:697–705.
Bretscher, M.S. 1996. Getting membrane flow and the cytoskeleton to cooperate in moving cells. *Cell*. 87:601–606.
Bright, N.A., B.J. Reaves, B.M. Mullock, and J.P. Luzio. 1997. Dense core lysosomes can fuse with late endosomes and are re-formed from the resultant hybrid organelles. *J. Cell Sci.* 110:2027–2040.
Coluccio, L.M. 1997. Myosin I. *Am. J. Physiol.* 273:C347–C359.
Damer, C.K., and T.J. O'Halloran. 2000. Spatially regulated recruitment of clathrin to the plasma membrane during capping and cell translocation. *Mol. Biol. Cell.* 11:2151–2159.
D'Souza-Schorey, C., E. van Donselaar, V.W. Hsu, C.Z. Yang, P.D. Stahl, and P.J. Peters. 1998. ARF6 targets recycling vesicles to the plasma membrane: insights from an ultrastructural investigation. *J. Cell Biol.* 140:603–616.
de Hostos, E.L., C. Rehfuess, B. Bradtke, D.R. Waddell, R. Albrecht, J. Murphy, and G. Gerisch. 1993. *Dictyostelium* mutants lacking the cytoskeletal protein coronin are defective in cytokinesis and cell motility. *J. Cell Biol.* 120:163–173.
Dunn, K.W., T.E. McGraw, and F.R. Maxfield. 1989. Iterative fractionation of recycling receptors from lysosomally destined ligands in an early sorting endosome. *J. Cell Biol.* 109:3303–3314.
Durrbach, A., D. Louvard, and E. Coudrier. 1996. Actin filaments facilitate two steps of endocytosis. *J. Cell Sci.* 109:457–465.
Durrbach, A., G. Raposo, D. Tenza, D. Louvard, and E. Coudrier. 2000. Truncated brush border myosin I affects membrane traffic in polarized epithelial cells. *Traffic*. 1:411–424.
Fujimoto, L.M., R. Roth, J.E. Heuser, and S.L. Schmid. 2000. Actin assembly plays a variable, but not obligatory role in receptor-mediated endocytosis in mammalian cells. *Traffic*. 1:161–171.
Futter, C.E., A. Gibson, E.H. Allchin, S. Maxwell, L.J. Ruddock, G. Odorizzi, D. Domingo, I.S. Trowbridge, and C.R. Hopkins. 1998. In polarized MDCK cells basolateral vesicles arise from clathrin-gamma-adaptin–coated domains on endosomal tubules. *J. Cell Biol.* 141:611–623.
Gaidarov, I., F. Santini, R.A. Warren, and J.H. Keen. 1999. Spatial control of coated-pit dynamics in living cells. *Nature Cell Biol.* 1:1–6.
Geli, M.I., and H. Riezman. 1996. Role of type I myosins in receptor-mediated endocytosis in yeast. *Science.* 272:533–535.
Geli, M.I., and H. Riezman. 1998. Endocytic internalization in yeast and animal cells: similar and different. *J. Cell Sci.* 111:1031–1037.
Gerisch, G., M. Maniak, and R. Neujahr. 1999. Patterns of cellular activities based on protein sorting in cell motility, endocytosis and cytokinesis. *Biochem. Soc. Symp.* 65:1–14.
Ghosh, R.N., D.L. Gelman, and F.R. Maxfield. 1994. Quantification of low density lipoprotein and transferrin endocytic sorting HEp2 cells using confocal microscopy. *J. Cell Sci.* 107:2177–2189.
Goodson, H.V., and J.A. Spudich. 1995. Identification and molecular characterization of a yeast myosin I. *Cell Motil. Cytoskeleton*. 30:73–84.
Gottlieb, T.A., I.E. Ivanov, M. Adesnik, and D.D. Sabatini. 1993. Actin microfilaments play a critical role in endocytosis at the apical but not the basolateral surface of polarized epithelial cells. *J. Cell Biol.* 120:695–710.
Griffiths, G., B. Burke, and J. Lucocq. 1993. Chapter 8. Particulate markers for immunoelectron microscopy. *In* Fine Structure Immunocytochemistry. Springer-Verlag, Berlin. 279–306.
Gruenberg, J., and F.R. Maxfield. 1995. Membrane transport in the endocytic pathway. *Curr. Opin. Cell Biol.* 7:552–563.
Hacker, U., R. Albrecht, and M. Maniak. 1997. Fluid-phase uptake by macropinocytosis in *Dictyostelium*. *J. Cell Sci.* 110:105–112.
Heuser, J., Q. Zhu, and M. Clarke. 1993. Proton pumps populate the contractile vacuoles of *Dictyostelium* amoebae. *J. Cell Biol.* 121:1311–1327.
Hirokawa, N. 1998. Kinesin and dynein superfamily proteins and the mechanism of organelle transport. *Science*. 279:519–526.
Hopkins, C.R., A. Gibson, M. Shipman, D.K. Strickland, and I.S. Trowbridge. 1994. In migrating fibroblasts, recycling receptors are concentrated in narrow tubules in the pericentriolar area, and then routed to the plasma membrane of the leading lamella. *J. Cell Biol.* 125:1265–1274.
Huber, L.A., I. Fialka, K. Paiha, W. Hunziker, D.B. Sacks, M. Bähler, M. Way, R. Gagescu, and J. Gruenberg. 2000. Both calmodulin and the unconventional myosin myr4 regulate membrane trafficking along the recycling pathway of MDCK cells. *Traffic*. 1:494–503.
Jenne, N., R. Rauchenberger, U. Hacker, T. Kast, and M. Maniak. 1998. Targeted gene disruption reveals a role for vacuolin B in the late endocytic pathway and exocytosis. *J. Cell Sci.* 111:61–70.
Jung, G., and J.A.I. Hammer. 1990. Generation and characterization of *Dictyostelium* cells deficient in a myosin I heavy chain isoform. *J. Cell Biol.* 110: 1955–1964.
Jung, G., C.J. Schmidt, and J.A.I. Hammer. 1989. Myosin I heavy-chain genes of *Acanthamoeba castellanii*: cloning of a second gene and evidence for the existence of a third isoform. *Gene*. 82:269–280.
Jung, G., X. Wu, and J.A.I. Hammer. 1996. *Dictyostelium* mutants lacking multiple classic myosin I isoforms reveal combinations of shared and distinct functions. *J. Cell Biol.* 133:305–323.
Kohtz, D.S., V. Hanson, and S. Puszkin. 1990. Novel proteins mediate an interaction between clathrin-coated vesicles and polymerizing actin filaments. *Eur. J. Biochem*. 192:291–298.
Kubler, E., and H. Riezman. 1993. Actin and fimbrin are required for the internalization step of endocytosis in yeast. *EMBO (Eur. Mol. Biol. Organ.) J.* 12: 2855–2862.
Lamaze, C., L.M. Fujimoto, H.L. Yin, and S.L. Schmid. 1997. The actin cytoskeleton is required for receptor-mediated endocytosis in mammalian cells. *J. Biol. Chem*. 272:20332–20335.
Lawson, M.A., and F.R. Maxfield. 1995. Ca2+- and calcineurin-dependent recycling of an integrin to the front migrating neutrophils. *Nature*. 377:75–79.
Lewis, A.K., and P.C. Bridgman. 1996. Mammalian myosin I alpha is concentrated near the plasma membrane in nerve growth cones. *Cell Motil. Cytoskeleton*. 33:130–150.
Linderman, J.L., and D.A. Lauffenburger. 1988. Analysis of intracellular receptor/ligand sorting in endosomes. *J. Theor. Biol.* 132:203–245.
Maniak, M. 1999. Green fluorescent protein in the visualization of particle uptake and fluid-phase endocytosis. *Methods Enzymol.* 302:43–50.
Maniak, M., R. Rauchenberger, R. Albrecht, J. Murphy, and G. Gerisch. 1995. Coronin involved in phagocytosis: dynamics of particle-induced relocalization visualized by a green fluorescent protein Tag. *Cell*. 83:915–924.
Mayor, S., J.F. Presley, and F.R. Maxfield. 1993. Sorting of membrane components from endosomes and subsequent recycling to the cell surface occurs by a bulk flow process. *J. Cell Biol.* 121:1257–1269.
McGoldrick, C.A., C. Gruver, and G.S. May. 1995. MyoA of *Aspergillus nidulans* encodes an essential myosin I required for secretion and polarized growth. *J. Cell Biol.* 128:577–587.
Mellman, I. 2000. Quo vadis: polarized membrane recycling in motility and phagocytosis. *J. Cell Biol.* 149:529–530.
Mermall, V., P.L. Post, and M.S. Mooseker. 1998. Unconventional myosins in cell movement, membrane traffic, and signal transduction. *Science.* 279:527–533.
Monnat, J., U. Hacker, H. Geissler, R. Rauchenberger, E.M. Neuhaus, M. Maniak, and T. Soldati. 1997. *Dictyostelium discoideum* protein disulfide-isomerase, an endoplasmic-reticulum resident enzyme lacking a KDEL-type retrieval signal. *FEBS Lett.* 418:357–362.
Mukherjee, S., and F.R. Maxfield. 2000. Role of membrane organization and membrane domains in endocytic lipid trafficking. *Traffic*. 1:203–211.
Müsch, A., D. Cohen, and E. Rodriguez-Boulan. 1997. Myosin II is involved in the production of constitutive transport vesicles from the TGN. *J. Cell Biol.* 138:291–306.
Nakagawa, H., and S. Miyamoto. 1998. Actin filaments localize on the sorting endosomes of 3Y1 fibroblastic cells. *Cell Struct. Funct.* 23:283–290.
Neuhaus, E.M., and T. Soldati. 1999. Molecular mechanisms of membrane trafficking. What do we learn from *D. discoideum*? *Protist.* 150:235–243.
Neuhaus, E.M., H. Horstmann, W. Almers, M. Maniak, and T. Soldati. 1998. Ethane-freezing/methanol-fixation of cell monolayers. A procedure for improved preservation of structure and antigenicity for light and electron microscopies. *J. Struct. Biol.* 121:326–342.
Nolta, K.V., J.M. Rodriguez-Paris, and T.L. Steck. 1994. Analysis of successive endocytic compartments isolated from *Dictyostelium discoideum* by magnetic fractionation. *Biochim. Biophys. Acta.* 1224:237–246.
Novak, K.D., and M.A. Titus. 1997. Myosin I overexpression impairs cell migration. *J. Cell Biol.* 136:633–647.
Novak, K.D., M.D. Peterson, M.C. Reedy, and M.A. Titus. 1995. *Dictyostelium* myosin I double mutants exhibit conditional defects in pinocytosis. *J. Cell Biol.* 131:1205–1221.
Ostap, E.M., and T.D. Pollard. 1996. Overlapping functions of myosin-I isoforms? *J. Cell Biol.* 133:221–224.
Padh, H., J. Ha, M. Lavasa, and T.L. Steck. 1993. A post-lysosomal compartment in *Dictyostelium discoideum*. *J. Biol. Chem*. 268:6742–6747.
Pagh, K., H. Maruta, M. Claviez, and G. Gerisch. 1984. Localization of two phosphorylation sites adjacent to a region important for polymerization on the tail of *Dictyostelium* myosin. *EMBO (Eur. Mol. Biol. Organ.) J.* 3:3271–3278.
Pierini, L.M., M.A. Lawson, R.J. Eddy, B. Hendey, and F.R. Maxfield. 2000. Oriented endocytic recycling of alpha5beta1 in motile neutrophils. *Blood*. 95:2471–2480.
Raposo, G., M.-N. Cordonnier, D. Tenza, B. Menichi, A. Dürrbach, D. Louvard, and E. Coudrier. 1999. Association of myosin I alpha with endosomes and lysosomes in mammalian cells. *Mol. Biol. Cell.* 10:1477–1494.
Rodriguez-Paris, J.M., K.V. Nolta, and T.L. Steck. 1993. Characterization of lysosomes isolated from *Dictyostelium discoideum* by magnetic fractionation. *J. Biol. Chem*. 268:9110–9116.
Schroer, T.A. 2000. Motors, clutches and brakes for membrane traffic: a commemorative review in honor of Thomas Kreis. *Traffic*. 1:3–10.
Schwarz, E., H. Geissler, and T. Soldati. 1999. A potentially exhaustive screening strategy reveals two novel divergent myosins in *Dictyostelium*. *Cell Biochem. Biophys.* 30:413–435.
Schwarz, E., E.M. Neuhaus, C. Kistler, A. Henkel, and T. Soldati. 2000. *Dictyostelium* myosin IK is involved in the maintenance of cortical tension and affects motility and phagocytosis. *J. Cell Sci.* 113:621–633.
Sheff, D.R., E.A. Daro, M. Hull, and I. Mellman. 1999. The receptor recycling

pathway contains two distinct populations of early endosomes with different sorting functions. *J. Cell Biol.* 145:123–139.

Shurety, W., N.L. Stewart, and J.L. Slow. 1998. Fluid-phase markers in the basolateral endocytic pathway accumulate in response to the actin assembly-promoting drug jasplakinolide. *Mol. Biol. Cell.* 9:957–975.

Slot, J.W., and H.J. Geuze. 1985. A new method of preparing gold probes for multiple-labelling cytochemistry. *Eur. J. Cell Biol.* 38:87–93.

Song, J., Z. Khachikian, H. Radhakrishna, and J.G. Donaldson. 1998. Localization of endogenous ARF6 to sites of cortical actin rearrangement and involvement of arf6 in cell spreading. *J. Cell Sci.* 111:2257–2267.

Souza, G.M., D.P. Mehta, M. Lammertz, J. Rodriguez-Paris, R.R. Wu, J.A. Cardelli, and H.H. Freeze. 1997. *Dictyostelium* lysosomal proteins with different sugar modifications sort to functionally distinct compartments. *J. Cell Sci.* 110:2239–2248.

Stoorvogel, W., V. Oorschot, and H.J. Geuze. 1996. A novel class of clathrin-coated vesicles budding from endosomes. *J. Cell Biol.* 132:21–33.

Stow, J.L., K.R. Fath, and D.R. Burgess. 1998. Budding roles for myosin II on the Golgi. *Trends Cell Biol.* 8:138–141.

Sussman, M. 1987. Cultivation and synchronous morphogenesis of *Dictyostelium* under controlled experimental conditions. *Methods Cell Biol.* 28:9–29.

Temesvari, L., J. Rodriguez-Paris, J. Bush, T.L. Steck, and J. Cardelli. 1994. Characterization of lysosomal membrane proteins of *Dictyostelium discoideum*. A complex population of acidic integral membrane glycoproteins, Rab GTP-binding proteins, and vacuolar ATPase subunits. *J. Biol. Chem.* 269:25719–25727.

Temesvari, L.A., J.M. Bush, M.D. Peterson, K.D. Novak, M.A. Titus, and J.A. Cardelli. 1996. Examination of the endosomal and lysosomal pathways in *Dictyostelium discoideum* myosin I mutants. *J. Cell Sci.* 109:663–673.

Thilo, L. 1985. Quantification of endocytosis-derived membrane traffic. *Biochim. Biophys. Acta.* 822:243–266.

Thilo, L., and G. Vogel. 1980. Kinetics of membrane internalization and recycling during pinocytosis in *Dictyostelium discoideum*. *Proc. Natl. Acad. Sci. USA.* 77:1015–1019.

Titus, M.A., D. Wessels, J.A. Spudich, and D. Soll. 1993. The unconventional myosin encoded by the myoA gene plays a role in *Dictyostelium* motility. *Mol. Biol. Cell.* 4:233–246.

Tuxworth, R.I., and M.A. Titus. 2000. Unconvetional myosins: anchors in the membrane traffic relay. *Traffic.* 1:11–18.

Uyeda, T.Q., and M.A. Titus. 1997. The myosins of *Dictyostelium*. *In Dictyostelium*: A Model System for Cell and Developmental Biology. Y. Maeda, K. Inouye, and I. Takeuchi, editors. Universal Academy Press, Tokyo, Japan. 43–64.

Vargas, M., H. Voigt, P. Sansonetti, and N. Guillen. 1997. Molecular characterization of myosin IB from the lower eukaryote *Entamoeba histolytica*, a human parasite. *Mol. Biochem. Parasitol.* 86:61–73.

Verges, M., R.J. Havel, and K.E. Mostov. 1999. A tubular endosomal fraction from rat liver: biochemical evidence of receptor sorting by default. *Proc. Natl. Acad. Sci. USA.* 96:10146–10151.

Weiner, O.H., J. Murphy, G. Griffiths, M. Schleicher, and A.A. Noegel. 1993. The actin-binding protein comitin (p24) is a component of the Golgi apparatus. *J. Cell Biol.* 123:23–34.

Wessels, D., J. Murray, G. Jung, J.A.I. Hammer, and D.R. Soll. 1991. Myosin IB null mutants of *Dictyostelium* exhibit abnormalities in motility. *Cell Motil. Cytoskeleton.* 20:301–315.